Int. J. Electrochem. Sci., 7 **(2012)** 13106 - 13120

International Journal of
ELECTROCHEMICAL
SCIENCE
www.electrochemsci.org

A New and Effective Macrocyclic compound as corrosion inhibitor for mild Steel in Hydrochloric Acid Solution

M.A. Quraishi[1*], *K.R Ansari*[1], *Eno E. Ebenso*[2]

[1] Department of Applied Chemistry, Indian Institute of Technology, Banaras Hindu University, Varanasi 221005, India
[2] Department of Chemistry, School of Mathematical and Physical Sciences, North-West University (Mafikeng Campus), Private Bag X2046, Mmabatho 2735, South Africa
[*]E-mail: maquraishi@rediffmail.com

Received: 29 October 2012 / *Accepted:* 16 November 2012 / *Published:* 1 December 2012

The inhibition characteristics of a macrocylic compound namely 1, 2, 4, 7, 9, 10-hexaazacyclo-pentadeca-10, 15-dien-3, 5, 6, 8-tetraone (HPTT) has been investigated on acid corrosion of mild steel in 1 M HCl using gravimetric measurement, electrochemical impedance spectroscopy (EIS) and potentiodynamic polarization. The maximum inhibition efficiency (η %) 95.2% of HPTT was obtained at 200 mgL^{-1}. Polarization curves indicate that HPTT acts as a mixed type inhibitor. The adsorption of inhibitor on mild steel surface followed Langmuir isotherm. Thermodynamic adsorption parameters such as adsorption heat (ΔH^{o}_{ads}), adsorption entropy (ΔS^{o}_{ads}) and adsorption free energy (ΔG^{o}_{ads}) have been calculated and discussed.

Keywords: Mild steel (MS); Corrosion inhibition; EIS; Adsorption.

1. INTRODUCTION

The use of inhibitors is an effective and economic method for protection of metallic corrosion. Organic compounds containing nitrogen, oxygen and sulphur atoms constitute an effective class of corrosion inhibitors [1-4]. Recently macrocylic compounds have emerged as new and potential class of corrosion inhibitors. A survey of literature reveals that, despite the high ability of the macrocylic compounds to interact strongly with metal surface, little attention has been focused on these compounds as corrosion inhibitors [5–8]. The corrosion inhibition occurs by the adsorption of these macrocyclics on to the metal surface which form a protective layer [9–11].In continuation of our work on development of macrocyclic compounds as a corrosion inhibitors[12-15] we report here the

inhibition properties of macrocylic compound namely 1,2,4,7,9,10-hexaazacyclo-pentadeca-10,15-dien-3,5,6,8-tetraone (HPTT) on corrosion of mild steel in 1 M HCl.

2. EXPERIMENTAL

2.1. Material preparation

The tested inhibitor was synthesized according to a previously described experimental procedure [12, 16]. The molecular structure of macrocyclic compound (HPTT) is shown in Figure 1.

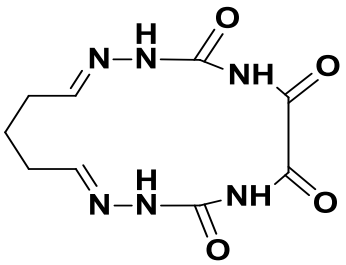

Figure 1. The molecular structure of macrocyclic compound (HPTT)

The Mild steel specimens, having composition (in wt %) 0.076 C, 0.012 P, 0.026 Si, 0.192 Mn, 0.050 Cr, 0.135 Cu, 0.023 Al, 0.050 Ni and the remainder iron were abraded successively with different grade emery papers (600 to 1200 grade), washed thoroughly with double distilled water and finally degreased with acetone and dried at room temperature. The test solution, 1M HCl was prepared by using of analytical grade HCl (37 %) and double distilled water.

2.2. Gravimetric measurements

Mild steel coupons of dimension (2.5 cm × 2.0 cm × 0.025 cm) were used for gravimetric studies. Weight loss measurement were performed by immersing mild steel coupons in conical flask containing 100 ml of HCl without and with different concentration of inhibitor. After the immersion time of 3h, mild steel (MS) coupons were taken out, washed with water, dried and weighted accurately using digital balance. The weight loss experiments were carried out from 308K to 338K. All experiments were carried out in static and deariated condition. The corrosion rate CR (mg cm^{-2} h^{-1}) from the following equation [17]:

$$C_R = \frac{W}{At} \quad (1)$$

where W is the average weight loss, A is the area of the mild steel coupons, t is the immersion time.

2.3. Electrochemical measurements

Electrochemical measurements were carried out using a GAMRY PCl4/300 electrochemical work station based on ESA400. Gamry applications include EIS300 (for EIS measurements) and DC105 software (for corrosion) and Echem Analyst (5.50 V) software for data fitting. All electrochemical experiments were performed in a Gamry three electrodes electrochemical cell under atmospheric condition. Platinum was used as the counter electrode and a saturated calomel electrode (SCE) as the reference electrode. Mild steel with the exposed area of 1.0 cm^2, was used as working electrode. Electrochemical measurements were carried out after 30 minutes to establish steady state OCP.EIS measurements were performed at corrosion potentials, E_{corr}, over a frequency range of 100 kHz to 10 mHz with an AC signal amplitude perturbation of 10 mV peak to peak. Potentiodynamic polarization studies were performed with a scan rate of $1mVs^{-1}$ in the potential range from -250 to +250 mVSCE versus OCP. Anodic and cathodic curves of the linear Tafel segment were extrapolated to corrosion potential to obtain corrosion current densities (I_{corr}).

3. RESULTS AND DISCUSSION

3.1. Gravimetric measurements

3.1.1. Effect of inhibitor concentration

Gravimetric measurements for the mild steel in 1M HCl solution in the absence and presence of different concentrations of macrocycle is given in the Table 1.

Table 1. Parameters obtained from gravimetric measurements for mild steel in 1 M HCl containing different concentrations of HPTT at 308 K

C_{inh} (mg/L)	C_R ($mg/cm^{-1}h^{-1}$)	θ	η (%)
Blank	7.0	-	-
50	1.33	0.809	80.9
100	0.93	0.866	86.6
150	0.50	0.928	92.8
200	0.33	0.952	95.2

From the table it is observed that as the concentration of the inhibitor increases inhibition efficiency (η %) increases and corrosion rate decreases. This is occurs due to increased adsorption and increased coverage of inhibitor on the mild steel surface.

3.1.2. Effect of temperature

The effect of temperature on the inhibition efficiency of the macrocycle for mild steel in 1 M HCl solution in the absence and presence of optimum concentration (200 mgL^{-1}) at temperature ranging from 308 to 338 K was investigated by weight loss measurements. The results obtained are given in Table 2 and plot between different temperature vs efficiency is shown in Figure 2.

Table 2. Parameters obtained from gravimetric measurements of mild steel in 1 M HCl containing optimum (200 mgL^{-1}) concentration of HPTT at different temperatures

Inhibitors	Temperature (K)	C_R ($mg/cm^{-1}h^{-1}$)	η (%)
Blank	308	7.0	--
	318	9.66	--
	328	14.6	--
	338	18.7	--
HPTT	308	0.33	95.2
	318	1.43	85.1
	328	4.70	67.8
	338	7.93	57.6

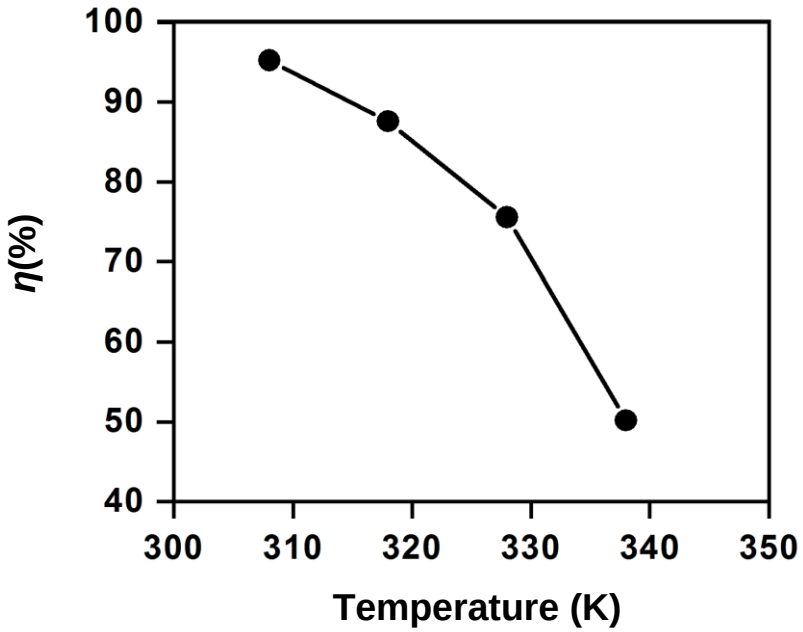

Figure 2. Variation of inhibition efficiency with Temperature

It is observed that as the temperature increases from 308 to 338 K inhibition efficiency decreases while corrosion rate increases. This behavior can be explained on the basis that the increase in temperature causes the desorption of the inhibitor molecules from the surface of mild steel. Table 2 shows that the corrosion rate increased with increasing temperature both in uninhibited and inhibited

solutions. In the absence of inhibitor corrosion rate increases with temperature. These results suggest that macrocycle acts as an efficient inhibitor for mild steel in 1 M HCl in the range of temperature (308-338) studied.

3.1.3. Effect of immersion time

The effect of immersion time on the inhibition efficiency is shown in Figure 3.

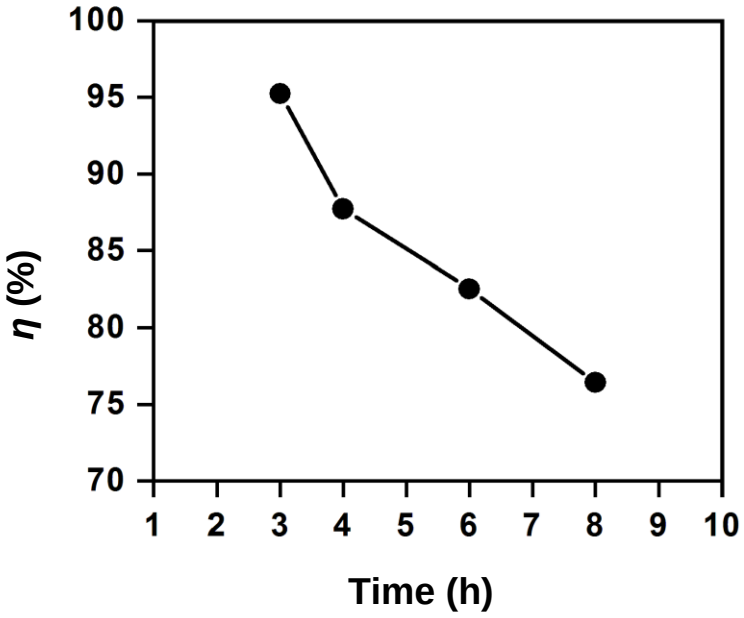

Figure 3. Variation of inhibition efficiency with Time

From the figure it is observed that inhibition efficiency decreases from 95.2 to 76.4 with time.

3.3.3. Thermodynamic activation parameters

A plot of the logarithm of the corrosion rate (mg cm^{-2} h^{-1}) of mild steel vs. 1000/T gave a straight line as shown in Figure 4.

The apparent activation energy (Ea) was calculated by using following Arrhenius equation:

$$C_R = A\exp\left(\frac{-E_a}{RT}\right) \quad (4)$$

where Ea is the apparent activation energy for the corrosion of mild steel in 1 M HCl solution, R gas constant, λ the Arrhenius pre-exponential factor and T is the absolute temperature. The values of Ea obtained from the slope of the line (Fig. 4) are given in Table 3.

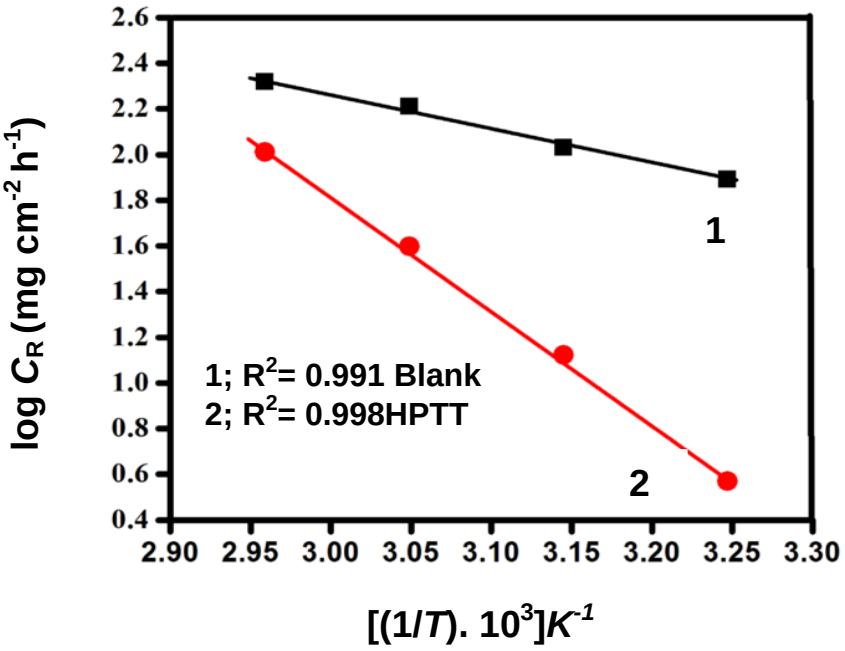

Figure 4. Arrhenius plot of mild steel in 1M HCl in absence and presence of different concentration of HPTT

Table 3. Thermodynamic parameters for mild steel in 1M HCl in absence and presence of optimum concentration of investigated inhibitor HPTT

Inhibitor	E_a (kJmol^{-1})	-ΔG^o_{ads} (kJ mol^{-1})				K_{ads} (10^3 M^{-1})				ΔH^o_{ads} (kJ mol^{-1})	ΔS_{ads} (J K^{-1}mol^{-1})
		308	318	328	338	308	318	328	338		
Blank	27.9	--	--	--	--	--	--	--	--	25.4	-147.4
HPTT	95.8	36.1	34.0	32.3	32.0	23.8	6.85	2.52	1.63	88.4	53.0

An alternative formula of the Arrhenius equation is the transition state equation:

$$C_R = \frac{RT}{Nh}\exp\left(\frac{\Delta S_a}{R}\right)\exp\left(-\frac{H_a}{RT}\right) \quad (5)$$

where N is the Avogadro's number, h the Planck's constant, ΔH° the enthalpy of activation and ΔS° the entropy of activation.

Figure 2 shows a plot of log (CR/T) versus 1000/T gives a straight line with a slope of (−ΔH°/2.303 R) and an intercept of log (R/Nh + ΔS°/2.303 R) from which the values of ΔH° and ΔS°are calculated and are given in Table 3 . The data reveals that the values of thermodynamic activation functions (E_a and ΔH°) of the corrosion of mild steel in 1MHCl solution in the presence of the inhibitor are higher than those in the free acid solution. Higher values of E_a and ΔH° in presence of

inhibitor indicate more energy is required for the dissolution of mild steel in 1 M HCl in presence of the macrocycle. The increase in the apparent activation energy for mild steel dissolution in inhibited solution may be interpreted as physical adsorption that occurs in the first stage [18]. The increase in activation energy can be attributed to an appreciable decrease in the adsorption of the inhibitor on the mild steel surface with increase in temperature.

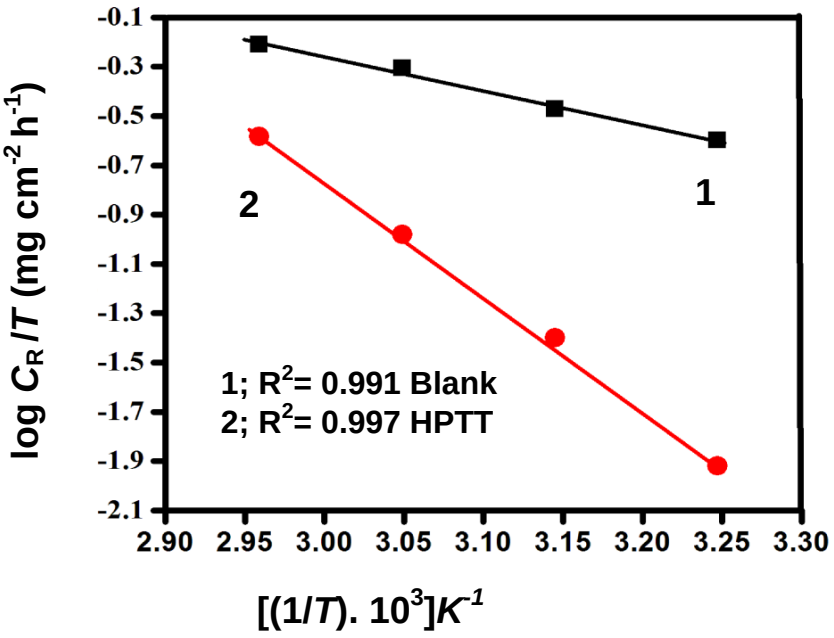

Figure 5. Transition-state plot of mild steel in 1M HCl in absence and presence of optimum concentration of HPTT

Inspection of Table 3 shows that value of enthalpy of activation is positive and higher in presence of inhibitor. The positive sign of ΔH° reflects the endothermic nature of the mild steel dissolution process suggesting that the dissolution of mild steel is slow. The entropy of activation ΔS° is higher (53.0K-1 mol-1) in presence of inhibitor than that (-147.4J K-1 mol-1) in the absence of the inhibitor. This is opposite to what would be expected, since adsorption of inhibitor is an exothermic process and is always accompanied by a decrease of entropy. The reason could be explained as follows: the adsorption of organic inhibitor molecules from the aqueous solution can be regarded as a quasi-substitution process between the organic compound in the aqueous phase [$Org_{(sol)}$] and water molecules at the electrode surface [$H2O_{(ads)}$]. In this situation, the adsorption of organic inhibitor is accompanied by desorption of water molecules from the surface. Thus, while the adsorption process for the inhibitor is believed to be exothermic and associated with a decrease in entropy of the solute, the opposite is true for the solvent. The thermodynamic values obtained are the algebraic sum of the adsorption of organic molecules and desorption of water molecules. Therefore, the gain in entropy is attributed to the increase in solvent entropy [19] The positive values of ΔS^0 means that the adsorption process is accompanied by an increase in entropy, which is the driving force for the adsorption of inhibitor onto the mild steel surface [20].

3.1.3. Adsorption considerations

The standard free energy of adsorption ($\Delta G°_{ads}$) at different temperatures is calculated from the equation:

$$\Delta G^{o}_{ads} = -RT \ln(55.5 K_{ads}) \quad (6)$$

where the value 55.55 is the concentration of water in solution expressed in M [17,21] and K_{ads} is equilibrium adsorption constant and is given by:

$$K_{ads} C = \frac{\theta}{1-\theta} \quad (7)$$

where θ is degree of surface coverage of the mild steel surface which is equals to E%/100 and C the molar concentration of inhibitor.

The values of adsorption equilibrium constant and standard free energy for mild steel in 1M HCl solution in the presence of 200 mgL^{-1}macrocycle is given in Table 3.

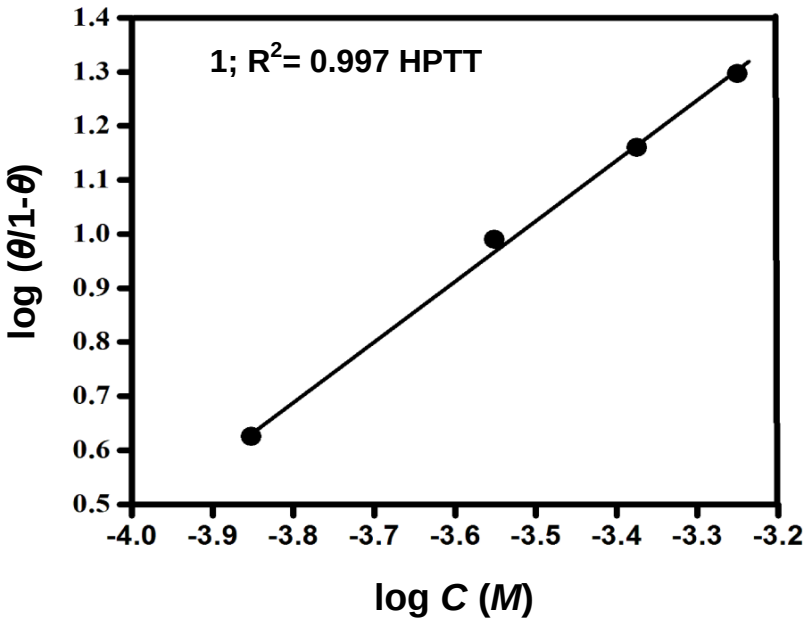

Figure 6. Langmuir's isotherm for adsorption of HPTT on mild steel surface in 1M HCl

The negative values of $\Delta G°_{ads}$ suggest that the adsorption of inhibitor molecules onto the mild steel surface is a spontaneous process [22].The large values of adsorption equilibrium constant also suggest the spontaneity of the adsorption process and stability of the adsorbed layer on the mild steel surface. Generally, accepted threshold value between chemisorption and physisorption for the $\Delta G°_{ads}$ is −40 kJ mol^{-1} [23]. The values of $\Delta G°_{ads}$ up to −20 $kJmol^{-1}$ are consistent with the electrostatic interaction between the charged molecules and the charged metal (physical adsorption) while those

more negative than −40 kJmol^{-1} involve sharing or transfer of electrons from the inhibitor molecules to the metal surface to form a coordinate type of bond (chemisorption) [24].The values of standard free energy of adsorption $\Delta G°_{ads}$) calculated in presence of the macrocycle are found to be slightly less negative than -40 kJ mol^{-1}. This probably suggests that the adsorption mechanism of the macrocycle on the mild steel surface in 1 M HCl solution involves chemisorption.

Several adsorption isotherms (such as Frumkin, Langmuir, Temkin, Freundlich, Bockris–Swinkels and Flory–Huggins isotherms) were used. But Langmuir adsorption isotherm was found to fit best with our experimental data. A straight line was obtained on plotting log θ/ (1− θ) vs. log C (mol L^{-1}) as shown in Figure 6.

It suggested that the adsorption of the inhibitor at the metal/ solution interface follows Langmuir's adsorption isotherm. The values of θ obtained from three different techniques are in good agreement and all obey the Langmuir adsorption isotherm.

3.2. Electrochemical measurements

3.2.3. AC technique: Electrochemical impedance spectroscopy

AC impedance results of mild steel/hydrochloric acid interface obtained in the absence and in the presence of various concentrations of macrocycle in the form of Nyquist plots are shown in Fig 7.

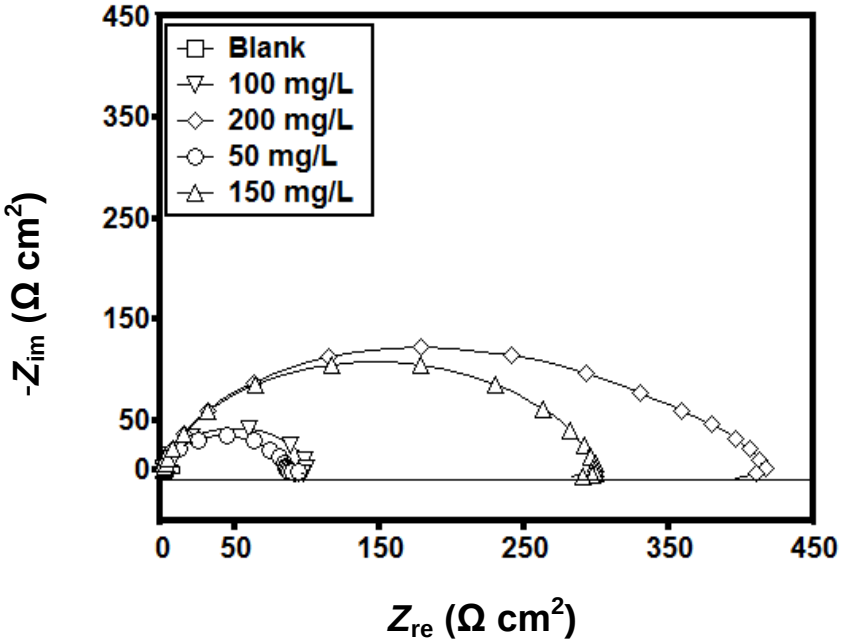

Figure 7. Nyquist plots for mild steel in 1M HCl in absence and presence of various concentrations of HPTT at 308 K

The Nyquist plots for all concentrations of macrocycle are characterized by one semicircular capacitive loop. The corrosion process is two steps as in any electrochemical process. First, the

oxidation of the metal (charge transfer process) and second, the diffusion of the metallic ions from the metal surface to the solution (mass transport process). Inhibitors get adsorbed on the electrode surface and thereby produce a barrier which inhibits corrosion. [25]

It must be noted that the capacitive loops are depressed ones with centers under the real axis even though they have a semicircle appearance. This kind of deviations is mostly referred to as frequency dispersion which is attributed to irregularities and heterogeneities of the solid surfaces [26]. In the real corrosion systems, the metal/solution interface double layer does not behave as a real capacitor. The charge distribution is controlled by electron on the metal side of the double layer, whereas it is controlled by ions on the solution side [27] The high frequency (HF) part of the impedance and phase angle reflects the behavior of heterogeneous surface layer, whereas the low frequency (LF) part shows the kinetic response for the charge transfer reaction [28]. A small inductive loop can be seen for both uninhibited and inhibited solutions (Figure 7). The presence of this low frequency inductive loop may be attributed to the relaxation process obtained by adsorption of species like $(Cl^-)_{ads}$ and $(H^+)_{ads}$ on the electrode surface [29]. The simplest model as shown in Figure 8.

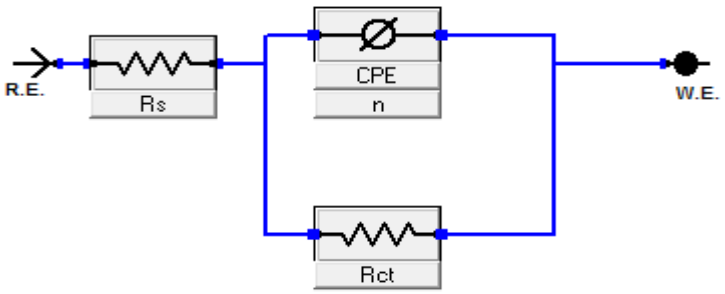

Figure 8. Equivalent circuit used to fit the EIS data

This consist of the solution resistance, R_s, in series with the parallel combination of constant phase element (CPE) in place of double layer capacitance (C_{dl}) and charge transfer resistance (R_{ct}).

Mathematically, a CPE's impedance is given by

$$Y_{\mathrm{CPE}} = Y_0(j\omega)^n \tag{8}$$

where Y_0 is the amplitude comparable to a capacitance, j is the imaginary unit, ω is the angular frequency (ω = 2πf, the frequency in Hz), and n is the phase shift gives details about the degree of surface in homogeneity. The CPE can be expressed by the values of n if resistance (n=0, Y0 = R), capacitance (n=1, Y0 = C), inductance (n= -1, Y0 = L) and Warburg impedance (n=0.5, Y0 = W) [30].

Simulated Nyquist and Bode plots with the above model showed excellent agreement with experimental data Figure 9 and 10.

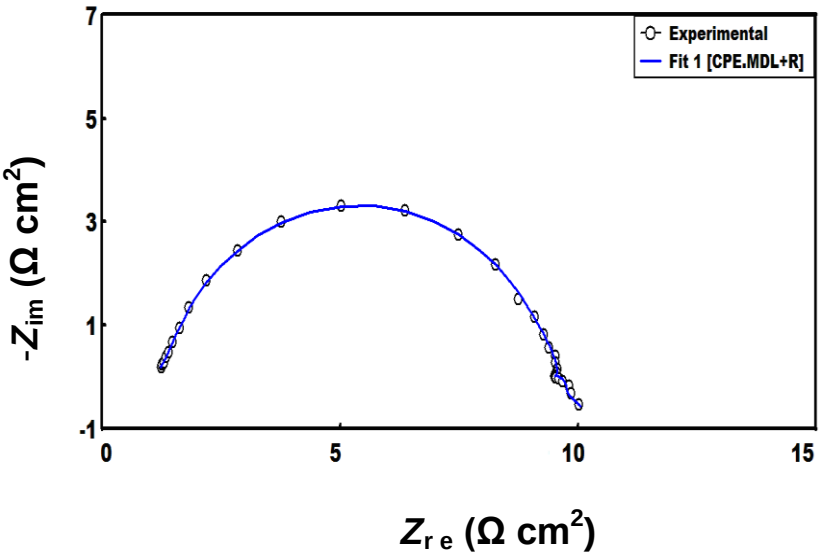

Figure 9. Simulated and experimentally generated Nyquist plot

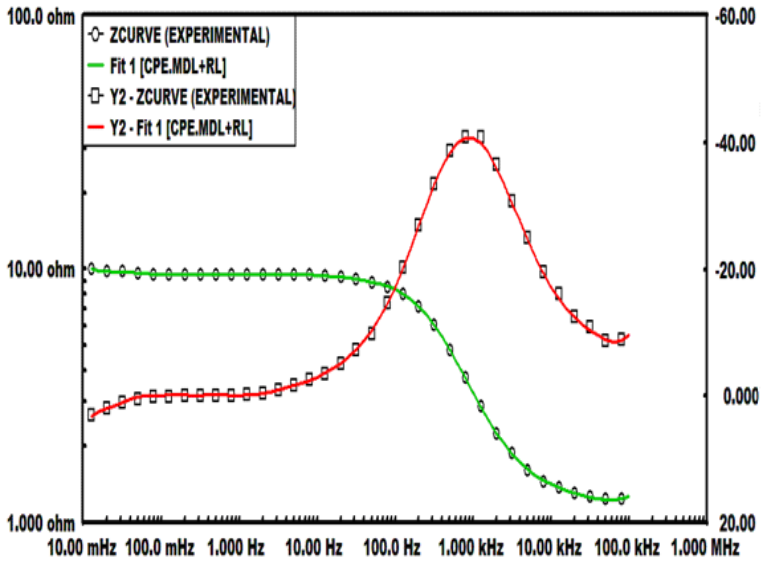

Figure 10. Simulated and experimentally generated Bode phase angle plots

The AC impedance parameters obtained from the Nyquist plots for mild steel in 1M HCl at different concentrations of macrocycle are given in Table 4.

Table 4 shows that the addition of the macrocycle in 1 M HCl increases the inhibition efficiency, charge transfer resistance and a decreases double layer capacitance (C_{dl}) given as [31]

$$C_{dl} = \frac{\varepsilon\varepsilon_0}{d} A$$

where ε_0 is the vacuum dielectric constant, ε is the local dielectric constant, d is the thickness of the double layer, and A is the surface area of the electrode. It is obvious hat the decrease in the C_{dl} values occurs due to the adsorption of macrocycle molecule on the metal surface. Decrease in the capacitance, which can result from a decrease in the local dielectric constant and/or an increase in the thickness of the electrical double layer, strongly suggests that the inhibitor molecules adsorbed at the metal/solution interface.

Table 4. Electrochemical parameters calculated form EIS measurements on mild steel electrode HCl in absence and presence of different concentration of HPTT at 308 K

C_{inh} (mgL^{-1})	R_s (Ω)	R_{ct} (Ω cm^2)	n	Y_0 ($\mu F/cm^2$)	C_{dl} ($\mu F/cm^2$)	η (%)
Blank	1.12	9.10	0.82	251.0	106.0	-
50	0.74	91.0	0.88	88.25	53.40	86.5
100	0.82	209.8	0.87	71.88	39.14	94.1
150	1.10	294.1	0.82	56.51	21.80	95.8
200	0.77	379.0	0.83	37.90	16.17	96.7

The Bode impedance magnitude and phase angle plots in the absence and presence of different concentration of inhibitor at its open circuit potential are shown in Figure.11 for mild steel electrode immersed in 1M HCl .

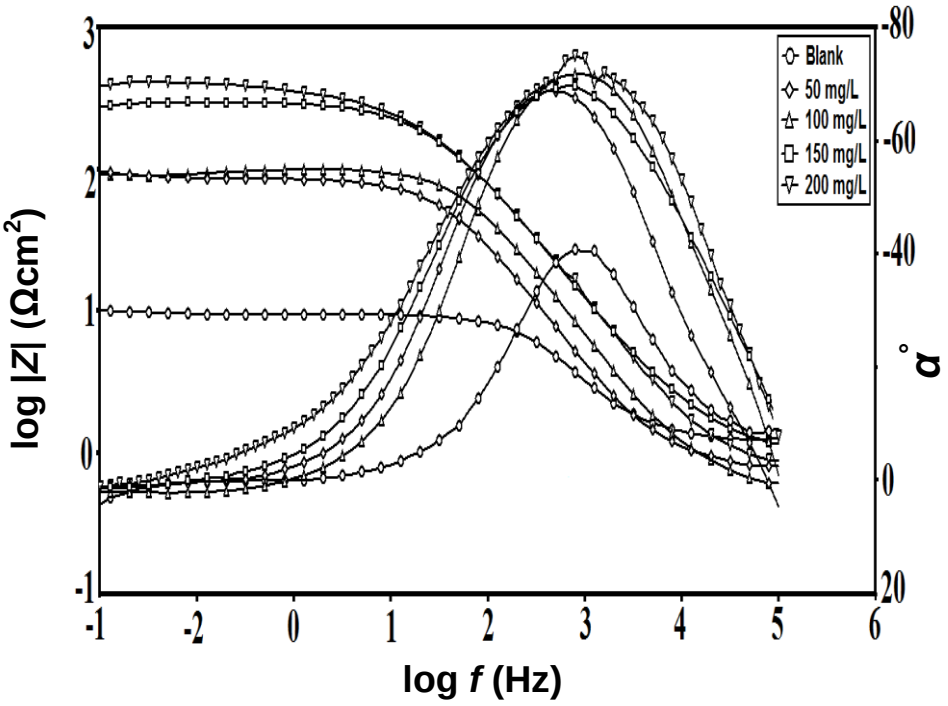

Figure 11. Bode impendence plots for mild steel in 1M HCl in absence and presence of various concentrations of HPTT at 308K

The values of maximum phase angles (α°) and Bode impedance magnitude (S) are listed in Table 5.

Table 5. The slopes of the Bode impedance magnitude plots at intermediate frequencies (S) and the maximum phase angles (α) for mild steel in 1M HCl solution at different concentration of HPTT at 308 K

C_{inh} (mgL^{-1})	$-S$	$-\alpha^{\circ}$
Blank	0.502	40.90
50	0.843	69.79
100	0.825	71.97
150	0.813	68.96
200	0.784	75.26

In the intermediate frequency region, a linear relationship between log |Z| against log f, with slope near -1 and the phase angle of -90◦, can be observed which is the characteristic of capacitive however an electrochemical system generally does not behave in an ideal manner [32]. The present study reveals that, in an intermediate frequencies region, a linear relationship between log |Z| vs. log f with a slope near -0.78 and the phase angle approaching -80° has been observed. This deviation occurs due to be the deviation from the ideal capacitive behavior at intermediate frequencies. The Bode phase angle plots show single maximum (one time constant) at intermediate frequencies, broadening of this maximum in presence of HPTT accounts for the formation of a protective layer on electrode surface [33].

3.2.2. Potentiodynamic polarization

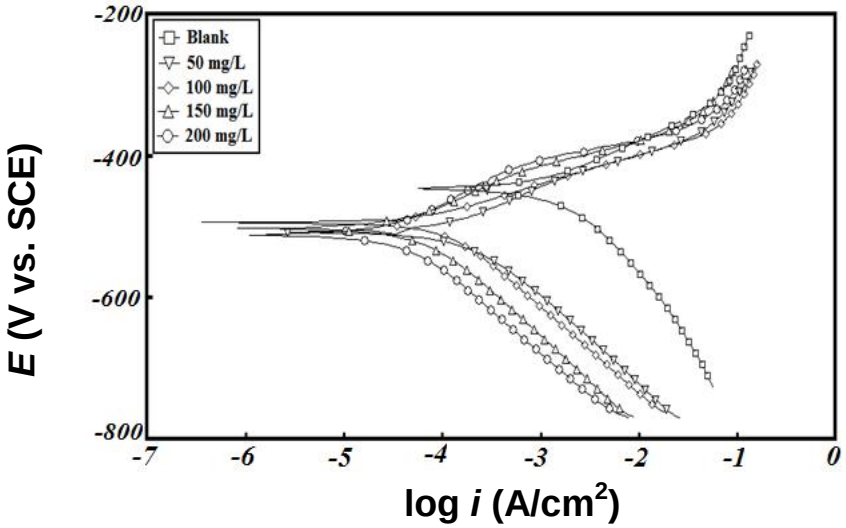

Figure 12. Potentiodynamic polarization curves for mild steel in 1M HCl in absence and presence of various concentrations of HPTT at 308 K

The Tafel polarization curves of mild steel in 1 M HCl in the absence and presence of different concentrations of macrocycle are shown in Figure 11.

The various electrochemical corrosion parameters, i.e. corrosion potential (E_{corr}), cathodic and anodic Tafel slopes (b_c, b_a) and corrosion current density (I_{corr}) obtained from the Tafel extrapolation of the polarization curves are given in Table 6.

It is seen from the tabulated data that the addition of macrocyclic compound decreases the corrosion current density from 892 μA/cm^2 to 42 μA/cm^2 thereby giving an efficiency of 96.1 at the concentration of 200 mgL^{-1}. The E_{corr} values are shifted by 67 mv towards negative direction thereby indicating that it is mixed inhibitor but predominantly acts as cathodic inhibitior. Similarly the change in b_c values are more pronounced than b_a which further corroborates the fact that it is predominantly a cathodic inhibitor.

Table 6. Potentiodynamic polarization parameters for mild steel in 1 M HCl solution in absence and presence of different concentration of HPTT at 308 K

C_{inh} (mg/L)	E_{corr} (mV/SCE)	I_{corr} (μA/cm^2)	b_a (mV/dec)	b_c (mV/dec)	η (%)
Blank	-444	892	61	81	–
50	-507	119	65	94	89.1
100	-493	82	48	105	92.5
150	-501	47	69	110	95.7
200	-511	42	91	120	96.1

4. MECHANISM OF INHIBITION

The mechanism of corrosion inhibition of mild steel in acidic solution by the HPTT macrocyclic compound can be explained on the basis of adsorption of HPTT on the metal surface. The adsorption on the inhibitor molecules on the mild steel surface is due to the donor atoms N, O of inhibitors and vacant d orbital's of the iron surface. HPTT molecules are macromolecules and can be adsorbed on the mild steel surface. Also it may lie flat on mild steel surface, hence block more surface area of the mild steel.

5. CONCLUSION

(1) Macrocyclic compound namely 1, 2, 4, 7, 9, 10-hexaazacyclo-pentadeca-10, 15-dien-3, 5, 6, 8-tetraone was found to inhibit corrosion of MS in 1M HCl. It showed high IE of 95.7% at a concentration of 200 mgL^{-1}.

(2) It was found to inhibit corrosion by adsorption mechanism.

(3) The adsorption of macrocyclic compound was found to obey Langmuir isotherm.

(4) Polarization study revels that it is a mixed type inhibitor but predominantly acts as cathodic inhibitor.

ACKNOWLEDGEMENT
The authors are grateful to Council of Scientific and Industrial Research (CSIR), New Delhi, India for providing financial help and support by granting research project under which this work has been done.

References

1. K.C. Pillai, R. Narayan, *Corros. Sci*. 2 (1983) 3
2. J.O'M. Bockris, J. McBreen, L. Nanis, J. *Electrochem. Soc.* 112 (1965) 1025
3. Bentiss, F. ,Traisnel, M.; Vezin, H.,Hildebrand, H,F, Lagrené, M. *Corros. Sci.* 46 (2004), 2781
4. M. Lagrené , B. Mernari, M. Bouanis, M . Traisnel, F. Bentiss, *Corros. Sci.* 44 (2002) 573
5. S. Hettiarachi, Y.W. Chan, R.B. Wilson, V.S. Agarwala, *Corrosion* 45 (1989) 30
6. F.R. Longo, J.J. Dellucia, V.S. Agarwala, in: Proceedings of the Sixth European Symposium on Corrosion Inhibitors, University of Ferrara, *Italy*, 1985, p. 155
7. V.S. Agarwala, *Proc. Int. Cong. Metallic Corros.* 1 (1984) 380
8. V.N.S. Pillai, J. Thomas, P.S. Harikumar, *Ind. J. Chem. Technol.* 2 (1995) 93
9. P.R. Roberge, *Handbook of Corrosion Engineering, McGraw- Hill,* 1999
10. F. Mansfled (Ed.), *Corrosion Mechanisms, Marcel Dekker, New York,* 1987
11. D. Jope, J. Sell, H.W. Pickering, K.G. Weil, *J. Electrochem. Soc.* 142 (1995) 2170
12. M. Ajmal, J Rawat, M.A. Quraishi, *Anti-Corrosion Methods and Materials*, U.K., 45 (1998), 419
13. M.A. Quraishi, J. Rawat, M . Ajmal. *Corrosion,* U.S.A., 54 (1998), 996
14. M. Ajmal, J. Rawat, M.A. Quraishi, *Bull. Electrochem*. 14 (1998), 199
15. M. A Quraishi, J. Rawat, *J. Electrochem. Soc.* 49 (2000), 35
16. N. Nishat, Rahisuddin ,S.Dhyani, *Journal of Coordination Chemistry*, 62, (2009), 996
17. X. Li, S. Deng, H. Fu, T. Li, *Electrochim. Acta.* 54 (2009) 4089
18. L. Larabi, O. Benali, Y. Harek, *Mater. Lett*. 61 (2007) 3287
19. B. Ateya, B. El-Anadauli, F. El Nizamy, *Corros. Sci.* 24 (1984) 509
20. XH .Li, SD. Deng, GN. Mu, H. Fu, FZ .Yang, *Corros. Sci.* 50 (2008) 420
21. E. Cano, JL. Polo, A. La Iglesia, JM. Bastidas, *Adsorption*. 10 (2004) 219
22. GK. Gomma, MH. Wahdan ,*Ind. J. Chem. Technol.* 2 (1995) 107
23. A. Yurt, S .Ulutas, H. Dal. *Appl. Surf .Sci.* 253 (2006) 919
24. E. Bensajjay, S. Alehyen, M. El Achouri, S .Kertit, *Anti-Corros Methods Mater* 50 (2003) 402
25. A.K. Satpati, P.V. Ravindran, *Mater. Chem. Phys.* 109 (2008) 352
26. K. Juttner, *Electrochim. Acta*. 35 (1990) 1501
27. M. Ozcan, I. Dehri, M .Erbil, *Appl. Surf. Sci.* 236 (2004) 155
28. MS. Morad, Corros. Sci. 42 (2000) 1307
29. HH. Hassan, E. Abdelghani, MA. Amin, *Electrochim. Acta* .52 (2007) 6359
30. K.F. Khaled, *Electrochim. Acta*. 55 (2010) 6523
31. EE. Oguzie, Y. Li, FH. Wang , *Electrochim. Acta.* 53 (2007) 909
32. H. H. Hassan, Electrochim. Acta. 53 (2007) 1722
33. K.R Ansari, Dileep Kumar Yadav, Eno E. Ebenso, M.A. Quraishi , *Int. J. Electrochem. Sci.*, 7 (2012) 4780